

Research Article

Laser Ablated Citrate-Stabilized Silver Nanoparticles Display Size and Concentration Dependant Biological Effects

Jelena Filipović Tričković , Miloš Momčilović , Gordana Joksić , Sanja Živković ,
Bojana Ilić , Miloš Ognjanović , Mirjana Novaković , and Ana Valenta Šobot 

VINČA Institute of Nuclear Sciences—National Institute of the Republic of Serbia, University of Belgrade, Belgrade, Serbia

Correspondence should be addressed to Ana Valenta Šobot; ana_v.s@vin.bg.ac.rs

Received 14 September 2022; Accepted 4 March 2023; Published 8 August 2023

Academic Editor: Raphael Schneider

Copyright © 2023 Jelena Filipović Tričković et al. This is an open access article distributed under the Creative Commons Attribution License, which permits unrestricted use, distribution, and reproduction in any medium, provided the original work is properly cited.

Silver nanoparticles (AgNPs) have been recognized for widespread biological applications due to their antimicrobial and anti-inflammatory effect, especially in dentistry and for wound healing. Many features determine their beneficial or toxic potential, such as their synthesis type, size, morphology, coating, and concentration. Most synthesis types rely on the use of synthetic chemicals, which contributes to their toxicity. We present an environmentally friendly method for “green” synthesis of AgNPs from the silver target by pulsed laser ablation in liquid (PLAL) using citrate as the stabilizing agent. Since AgNPs already have many dental applications, we examined their antibacterial effect against supragingival biofilm-forming bacteria and bacterial strains known to cause resistant dental infections. Their impact on human fibroblast cells’ cytotoxicity, proliferation (measured by XTT and Ki-67 immunofluorescence), pro/antioxidant balance, and lipid peroxidation (measured by PAB and LPP) was evaluated. AgNPs1 (21 nm) and AgNPs2 (15 nm) spherical nanoparticles with good overall stability were obtained. The highest tested dose of smaller nanoparticles (AgNPs2) displays not only an effective antibacterial effect against the tested oral bacteria strains but also a pro-oxidant and cytotoxic effect on fibroblast cells. Lower doses do not affect bacterial survival but increase the cell proliferation and metabolic activity and show an antioxidative effect, suggesting that different concentrations display a substantially opposite effect. Compared to larger AgNPs1, smaller AgNPs2 possess more potent biological effects, indicating that size plays a pivotal role in their activity. Such opposite outcomes could be important for their medical application, and high concentrations could be used for the inhibition of dental biofilm formation and resistant dental infections as well as proliferative conditions, while low doses could be beneficial in the treatment of atrophic and inflammatory disorders. Finally, we showed that silver-targeted PLAL, using citrate as a stabilizing agent, produces biologically potent nanoparticles that could have many applications depending on their size and concentration.

1. Introduction

Silver nanoparticles (AgNPs) have been extensively studied over the past decades as a promising agent in various fields, from the food and paint industry to the wide spectrum of medical applications such as wound healing, material coating, dentistry, or even as potential anticancer agents [1–5]. Most of these applications rely on their well-known anti bacterial [6] and biofilm inhibitory activities, antifungal, anti-viral, anti-inflammatory, antiangiogenic, and anticancer agents [7], as well as antiparasitic, antioxidant, and

anticoagulant activities [8]. On the other hand, the apparent adverse effects of AgNPs have also been reported, varying from cyto- and genotoxicity, neurotoxicity, cardiotoxicity, and nanoparticle-induced oxidative stress [9]. Several mechanisms have been described to contribute to AgNPs-induced toxicity. The induction of oxidative stress is one of the major mechanisms responsible for the antibacterial effects of AgNPs and also its geno- and cytotoxicity [10–13]. It has been reported that AgNPs increase the oxidative stress by ROS generation and antioxidant enzymes inhibition, which leads to lipid, DNA, and protein oxidative damage

[14]. These effects combined with proliferation suppression are considered to be the main causes of AgNPs-induced cytotoxicity. Also, the literature data indicate that AgNPs could also lead to enhanced cell proliferation and have overall beneficial effects on human cells [2, 15]. It appears that many features determine their toxic or beneficial potential, such as their size, morphology, dose, crystallinity, agglomeration, surface coating, and synthesis type [9, 16–20]. The synthesis type and the nanoparticle size were proven to be the major factors affecting nanoparticle-induced toxicity [9]. Among the many types of AgNPs synthesis the most common are chemical—using silver nitrate as a precursor and various reducing agents as a stabilizer; green—using natural precursors such as plant extracts [21, 22], bacteria, enzymes, electrochemical, and photochemical [23]. Chemically synthesized AgNPs are demonstrated to have the most toxic effects since synthetic chemicals are used as reducing agents, such as sodium borohydride and dimethylformamide [16]. On the other hand, laser synthesis from a metal target by pulsed ablation in liquid (PLAL) is the method that avoids the use of hazardous chemicals while simultaneously allowing the formation of stable nanoparticles [24]. The antibacterial effect of nanoparticles synthesized in this manner is relatively rarely investigated although it is believed to possess bactericidal potential without uncontrollable parameters [25, 26]. The liquid used for the synthesis could be supplemented with capping or stabilizing molecules. Among those, citric acid or sodium citrate is considered to be effective in size and shape control throughout the synthesis process, generation of monodispersed nanoparticles, and act as both reducing and stabilizing agents [27]. Its main advantage is the possibility of further AgNPs functionalization due to the highly negatively charged surface and weak interaction of citrate molecules with metal surfaces and because of this, they can be easily exchanged by many other molecules or ligands [28]. However, capping or stabilizing molecules can affect the biological response to nanoparticles directly or indirectly through the modulation of their physicochemical characteristics, with regards to their toxicity [29]. Therefore, our study aimed to evaluate the biological effects of laser ablated AgNPs synthesized with the addition of citric acid and using different laser energies. Since AgNPs have already found significant topical prophylactic or therapeutic use in dentistry in recent years, [5, 30] the investigation of laser ablated citrate-stabilized AgNPs antibacterial effects on oral contaminants could provide important findings for their further application. For this purpose, we have chosen bacteria commonly involved in supragingival dental biofilm formation, [31, 32] as well as bacterial strains that may be responsible for the failure of the different dental infection treatments [33].

Additionally, considering reported adverse effects of AgNPs that are not negligible, [9–14] their effect on the human fibroblasts regarding cytotoxicity as well as proliferation suppression and their relation to oxidative stress parameters were also determined.

2. Materials and Methods

2.1. AgNPs Synthesis. AgNPs were produced by the laser ablation method. A high purity (>99.99% metal basis, 1.0 mm thick, Alfa Aesar, USA) silver foil was placed in a glass and covered with 6 mL of deionized water and 200 μ L of a 0.6 mg/L water solution of citric acid (citric acid monohydrate p.a., Alkaloid Skopje). Before ablation, the silver plate was cleaned by using an ultrasonic bath for 30 minutes to remove contamination. The laser applied was the picosecond Nd:YAG system (Nd:YAG EKSPILA SL 212/SH/FH, LT), operating at the fundamental wavelength of 1064 nm with a 150-ps pulse length, pulse energies were 6 mJ (further referred to as AgNPs1) and 12 mJ (further referred to as AgNPs2), giving fluencies of 0.12 and 0.24 J/cm², respectively. During the irradiation, the laser was focused on the Ag target using a 16 cm lens. Each sample was irradiated for 20 minutes at room temperature, leading to the formation of a pale-yellow colloidal suspension.

2.2. AgNPs Characterization. To determine the nanoparticles' concentration, size, shape, composition and structure, several measurements were performed. First of all, the total concentration of silver in these colloidal solutions was determined using the ICP-OES method (ICP-OES, iCap7400 DUO, Thermo Fisher, USA). The ultraviolet-visible spectrum of AgNPs colloidal solutions was recorded in the wavelength range from 190 to 1100 nm using a UV-Vis spectrophotometer (LLG-UNISPEC 2, LLG Labware, USA).

The size, shape, and dispersity of Ag nanoparticles were analysed by transmission electron microscopy (TEM), using a FEI Talos F200X microscope at 200 keV with an X-FEG source and point-to-point resolution below 0.24 nm. The micrographs were captured in the conventional mode and recorded on a CCD camera with a resolution of 4096 \times 4096 pixels using the User Interface software package. The samples for TEM examination were prepared by a standard procedure in which a drop of the very dilute suspension was placed on a carbon-coated copper grid, which was allowed to dry in the air.

The size distributions were determined by manually measuring 60–120 particles using the public domain software ImageJ [34]. For obtaining the mean particles' size (d_{TEM}) and an index of polydispersity (PdI), the collected data were finally fitted to a log-normal function as follows:

$$y = y_0 + \frac{A}{\sqrt{2\pi\omega x}} e^{-[\ln(x/x_c)]^2/2\omega^2}. \quad (1)$$

The averaged hydrodynamic diameters (d_H) were estimated by dynamic light scattering (DLS), measured on a NanoZS90 apparatus (Malvern, UK) with a 4 mW He-Ne laser source ($\lambda = 633$ nm). The measurements were performed in disposable polystyrene cuvettes (DTS0012) at ambient temperature ($25 \pm 0.1^\circ\text{C}$).

2.3. Determination of Minimal Inhibitory Concentration (MIC). The antimicrobial activity of AgNPs in comparison to standard was investigated on bacterial strains responsible for the formation of supragingival dental biofilm such as *Streptococcus mutans* (ATCC 25175), *Aggregatibacter actinomycetemcomitans* (ATCC 29552), *Porphyromonas gingivalis* (ATCC 33277), *Fusobacterium nucleatum* (ATCC 25586), as well as on bacteria responsible for the failure of the treatment of different dental infections: *Staphylococcus aureus* (ATCC 25923), *Escherichia coli* (ATCC 25922), *Pseudomonas aeruginosa* (ATCC 27853), and *Streptococcus β haemolyticus* (ATCC 27956) using the microdilution method according to ISO20776-1. The aerobic bacterial stock was cultured on Mueller–Hinton Agar (HiMedia Laboratories, Dindhori, India) at 37°C for 24 hours, while the anaerobic stocks were cultured on the Shaedler broth (Thermo Fisher Scientific, Waltham, MA, USA) with vitamin K and hemin at 37°C for 72 hours in an anaerobic chamber.

After being cultured, the bacterial strains were suspended in sterile saline to obtain the final cell concentration of 5×10^5 CFU/mL. The minimum inhibitory concentrations (MICs) were determined after 24 hours of incubation of two-fold serial dilutions of the investigated samples (100 μ L) prepared in the liquid growth medium inoculated with bacterial strains using 96-well plates under aseptic conditions. The plates that did not contain the investigated samples were used as controls.

2.4. Cell Culture and Treatment. The human primary dermal fibroblast cell line (PCS-201-012™) was commercially available (<https://www.atcc.com>). The cells were grown in Dulbecco's modified eagle's medium (DMEM, Gibco, Thermo Fisher Scientific, USA) supplemented with 10% heat-inactivated fetal bovine serum (FBS, Capricorn Scientific, Germany) at 37°C and 5% CO₂. The cell cultures were treated in the log phase and at the subconfluence level, with four concentrations of AgNPs determined MIC concentration (results section) and three lower concentrations of 0.05, 0.1, and 1 ppm (parts per million) for 24 hours.

2.5. XTT Assay. The viability assay (XTT) was performed according to the standard procedure [35]. Shortly, after treatment and medium discharge, the cultured cells were supplemented with XTT reagent activated with phenazine methosulfate (PMS) and placed at 37°C until the colour developed. Absorbance was measured at 470 nm on a microplate reader (Sunrise, Tecan Group Ltd., Switzerland).

2.6. Ki-67 Immunofluorescence. Ki-67 immunofluorescent staining was performed to elucidate the effects of AgNPs not only on cellular survival but also on the proliferation rate. To perform immunofluorescent staining, the cells were grown on polylysine-coated slides (Merk, Germany) and after adhering to the polylysine surface, treated with AgNPs for 24 hours. After the treatment, the cells were fixed with 4%

formaldehyde solution in 1 x PBS, permeabilized with 0.25% Triton-X (Merk, Germany), and blocked with 1% BSA solution. Directly labelled Ki-67 (SolA15, FITC, eBioscience™, Thermo Fisher Scientific, USA) antibody was hybridized overnight at 4°C. The slides were washed in 1 x PBS solution, dehydrated in series of ethanol, and stained using DAPI-Vectashield solution (Vector laboratories, United Kingdom). The results are presented as the proliferative index (PI), the ratio between immunoreactive (Ki-67+) cells, and the total number of cells. At least 500 cells per treatment were analysed using a Zeiss-Axioimager A1 microscope and the ISIS imaging software package (MetaSystems, Altlußheim, Germany).

2.7. Pro-Oxidant/Antioxidant Balance (PAB) Assay. Following 24 hours of treatment, the medium was discarded, and cells were detached from the flasks using the trypsin solution (0.5% Trypsin-EDTA, Capricorn Scientific, Germany). After washing with PBS, the cells were lysed by repeated freezing and thawing. Results for both the PAB assay and lipid peroxidation products were presented per mg of proteins in the samples, according to Lowry [36].

PAB assay was performed as previously described in [37]. Two oxidation-reduction processes in the same sample are in the basis of the following assay: oxidation of chromogen 3,3',5,5'-tetramethylbenzidine (TMB) to a coloured cation by peroxides, catalysed by the horseradish peroxidase (HRP), and a reduction of coloured cation by antioxidants to a colourless compound. The optical density (OD) of the coloured product was measured at 450 nm, with a reference wavelength of 570 nm. The values are presented as arbitrary Hamidi-Koliakos (HK) units and calculated from the standard curve of H₂O₂ in the standard solution.

2.8. Lipid Peroxidation Products (LPP). The LPP assay relies on the reaction of *N*-methyl-2-phenylindole with lipid peroxidation products, malondialdehyde (MDA), and 4-hydroxyalkenals (HNE) [38]. This reaction produces a stable chromophore with an OD value of 586 nm. LPP values were calculated as equivalents of the 1,1,3,3-tetramethoxypropane standard curve.

2.9. Statistical Analysis. Experiments were set up in triplicate and repeated twice. The results were presented as means \pm standard error of the mean (SEM). The one-way ANOVA statistical test was used for statistical analysis using SPSS 10 for Windows (IBM, Armonk, NY, USA). The level of significance was set to <0.05.

3. Results and Discussion

3.1. AgNPs Synthesis and Characterization. Two different laser energies applied during the laser ablation of silver foil led to two types of nanoparticles, whose size and concentration were different; AgNPs1 (laser energy: 6 mJ) and AgNPs2 (laser energy: 12 mJ). The concentrations of AgNPs were 17.4 ± 0.1 and 28.7 ± 0.2 μ g/mL for AgNPs1 and

AgNPs2, respectively. UV-Vis spectroscopy is the simplest way to confirm the formation of nanoparticles. The appearance of a peak near 430 nm (Figure 1) demonstrates the surface plasmon resonance properties of AgNPs [39]. Also, there is a clear enhancement in the intensity of the surface plasmon resonance (SPR) band with the increasing nanoparticle concentration.

The morphology and particle size were obtained by statistical analysis of prepared nanoparticles. Typical TEM micrographs of AgNPs1 and AgNPs2 are shown in Figures 2(a) and 2(b). The nanoparticles are mainly spherical and pseudospherical, with larger particles tending to form hexagonal shapes. The particles are partially agglomerated on each other, and their sizes are subjected to the log-normal size distribution (Figures 2(c) and 2(d)). After the statistical analysis, the mean particle size of AgNPs1 was $d_{TEM} = 21.2 \pm 6.8$ nm (the polydispersity index was 32.1%), while the size of AgNPs2 was $d_{TEM} = 15.3 \pm 4.6$ nm ($PdI \approx 30\%$).

As is generally accepted, the very negative zeta potential of nanoparticles indicates their good colloidal stability [16]. Furthermore, zeta potential values for colloidal suspensions stabilized by electrostatic repulsion must be at least ± 30 mV [40]. The zeta potentials of the produced silver colloidal solutions were -32.1 ± 5.22 mV and -33.2 ± 5.61 mV for AgNPs1 and AgNPs2, respectively.

The hydrodynamic diameters of nanoparticles' aqueous suspension at pH 7 were determined by the DLS method (Figure 2). The obtained d_H values for AgNPs1 and AgNPs2 were 81 ± 19 nm and 78 ± 18 nm, respectively. The difference between the measured d_{TEM} and d_H is because the d_H value presents the size of the nanoparticles in their hydrated state, together with the surrounding layers of water molecules that extend the hydrodynamic diameter and make the hydrated shell around the particle significantly larger than the particles themselves. Unlike DLS, this cannot be observed by microscopic techniques because of the low background originating from low electron density. The measured d_H values of synthesized nanoparticles were notably higher than the d_{TEM} , which may be a hint of a certain degree of particles' agglomeration in suspension. That can lead to an unwanted destabilization of the colloid. Nevertheless, the obtained d_H values were still inside the acceptable biomedical application range (less than 100 nm).

3.2. Determination of Minimal Inhibitory Concentration (MIC). MICs represent the lowest concentration of samples that completely inhibit visible bacterial growth. AgNPs2 with a higher concentration and smaller particle size (15.3 ± 4.6 nm) showed antibacterial potential at $14.35 \mu\text{g}/\text{mL}$ against all tested oral pathogens (*Streptococcus mutants*, *Aggregatibacter actinomycetemcomitans*, *Porphyromonas gingivalis*, and *Fusobacterium nucleatum*) as well as one gram-positive (*Staphylococcus aureus*) and one gram-negative bacteria *Pseudomonas aeruginosa*, but had no effect against *Escherichia coli* and *Streptococcus β haemolyticus*. Unlike AgNPs2, AgNPs1 did not display an antibacterial effect against any of the tested bacteria, not even when concentrated.

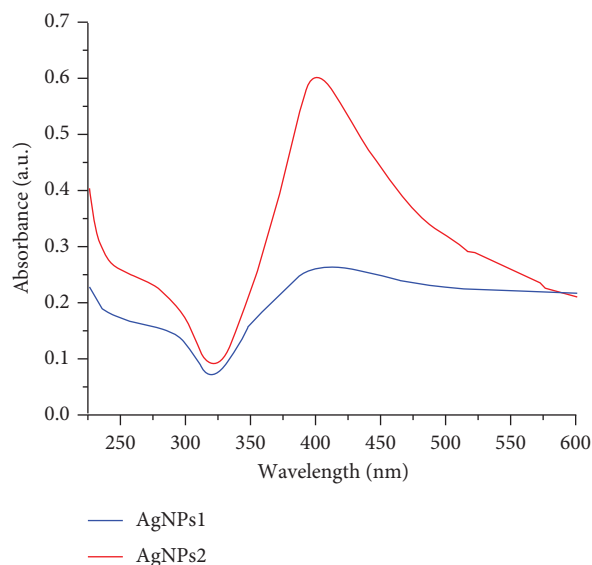


FIGURE 1: The typical UV-VIS photoabsorption spectrum of AgNPs exhibits a prominent characteristic peak at about 430 nm.

Antibacterial effects of AgNPs against all tested oral pathogens, as well as *Pseudomonas aeruginosa* and *Staphylococcus aureus* have previously been reported in the literature, whereas reported minimal inhibitory concentrations varied to a great extent from approximately 5 to $50 \mu\text{g}/\text{mL}$, depending on the tested strain, clinical or commercial, as well as the nanoparticle size [41]. Also, all of these nanoparticles were chemically synthesized, where toxic waste is produced during the synthesis process and could have a synergistic effect with the silver. Barabadi et al. (2021) compared the antibacterial effects of photo-synthesized AgNPs using the *Zataria multiflora* plant extract (green synthesis) with commercially available and chemically synthesized citrate-reduced AgNPs against *Staphylococcus aureus* and *Pseudomonas aeruginosa*. They stated that green synthesized AgNPs had the most potent antibacterial effects against tested bacterial strains in planktonic, as well as in the biofilm form [42]. Hamida et al. reported similar findings when compared biogenic AgNPs and silver nitrate. They found out that the effects are a result of intracellular ROS generation leading to biomolecules oxidation [43]. Reduction in ATP levels in AgNPs-treated bacteria support these findings [44]. However, reports on the antimicrobial activity of laser synthesized AgNPs are rather limited, [24, 41, 45, 46] and to the best of our knowledge, they are not available for the oral pathogens.

Since undiluted AgNPs1 have greater concentration than MIC for AgNPs2, the probable reason for AgNPs2 efficacy is the smaller particle size. Other research groups have also reported that the antimicrobial effect of AgNPs correlates with smaller particle sizes and nanoparticle shape [41, 47, 48]. Since both synthesized nanoparticles are similar in shape (spherical and pseudospherical), the size seems to be the determining factor for the antibacterial activity in this case. Comparing AgNPs with different sizes, shapes, and

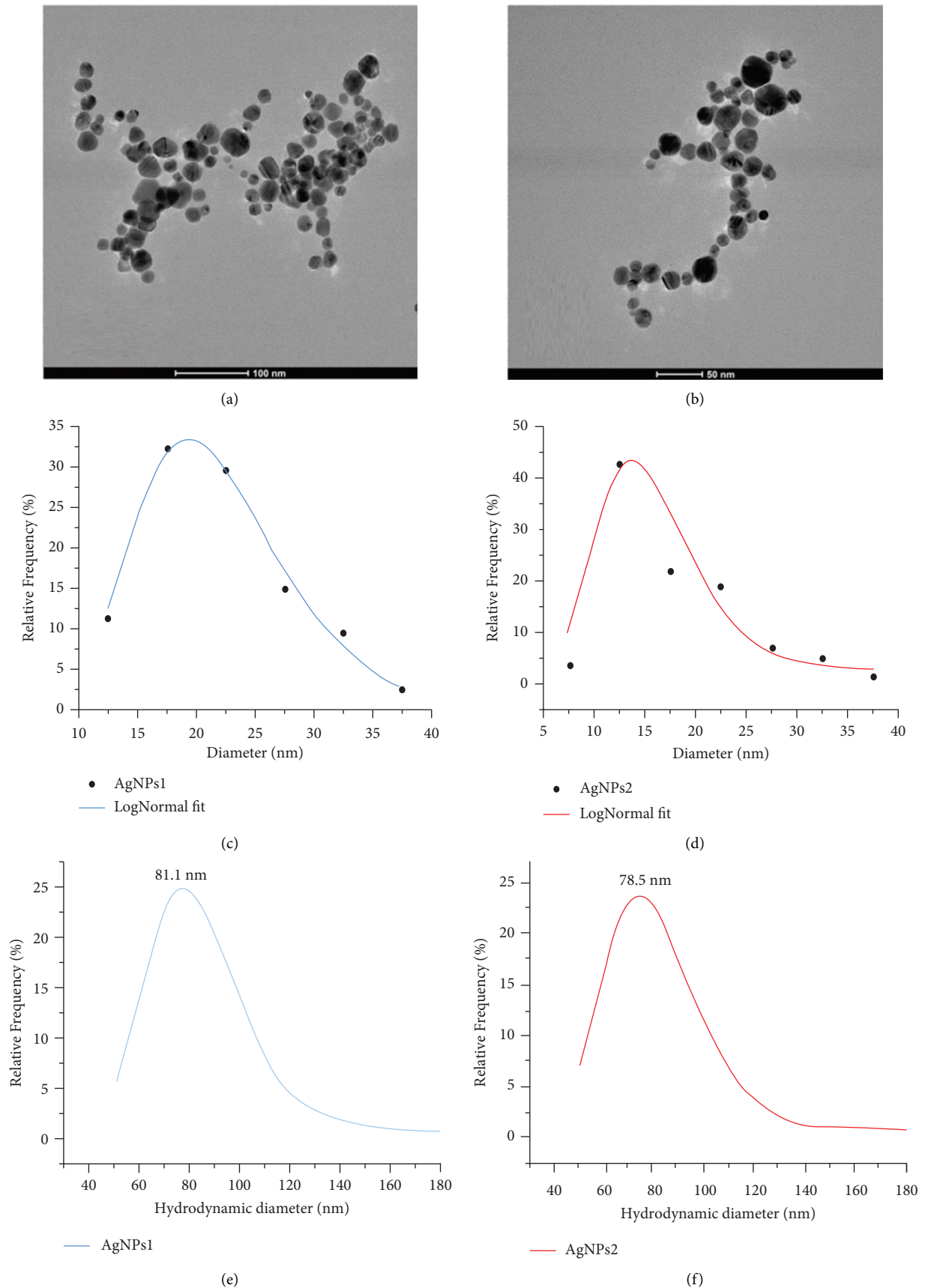


FIGURE 2: (a) TEM micrograph of AgNPs1 nanoparticles; the scale bar is 100 nm; (b) TEM micrograph of AgNPs2 nanoparticles; the scale bar is 50 nm; (c-d) corresponding log-normal particle size distributions. Hydrodynamic diameters of AgNPS1 (e) and AgNPS1 (f) measured by the DLS method.

surface coatings revealed that shape had a greater influence on the antibacterial activity than surface coatings [49]. Besides size, shape, and concentration, other factors could contribute to their antimicrobial effects, such as direct bacterial cell membrane damage, protein and/or enzyme inhibition and denaturation, and the generation of reactive oxygen species (ROS) with subsequent oxidation of the cellular macromolecules [6, 9, 50]. Apparently, ROS production plays a major role in the antimicrobial activity since it was demonstrated that it interacts with thio redoxin system of *Staphylococcus aureus*, one of the most important systems in the processes of oxidative stress. This interaction leads to depletion of intracellular thiol which in turn activates the oxidative stress by the disruption of the protective components [51]. The proposed antibacterial mechanisms of AgNPs are presented in Figure 3.

3.3. PAB, LPP, Cellular Survival, and Proliferation. To determine nanoparticle effects on ROS production and their effects on the redox state and macromolecules on the human fibroblast cell line, we measured prooxidant/antioxidant balance and formation of lipid peroxidation products after 24 hours treatment with MIC concentration (14.35 $\mu\text{g}/\text{mL}$) of both AgNPs1 and AgNPs2. We also used smaller concentrations of 1, 0.1, and 0.05 $\mu\text{g}/\text{mL}$ to examine the effects of low concentrations and concentration dependence. The highest tested concentration of both nanoparticles induced significant elevations of PAB and LPP values ($p < 0.001$). Comparing the effects of two types of synthesized nanoparticles, the increase was significantly higher after AgNPs2 treatment for PAB values ($p < 0.001$, Figure 4).

These results are consistent with the literature data, where the antibacterial effects of AgNPs are mostly attributed to the generation of ROS [52]. The higher pro-oxidant state and increased lipid peroxidation products after AgNPs2 treatment suggest that the particle size plays a pivotal role in ROS production, which is mostly accredited to the larger surface areas that enable interaction with the cellular macromolecules [17]. Consistent with these results are the effects on cellular survival and proliferation. The same concentration of AgNPs led to a dramatic loss of viable cells compared to the control ($p < 0.001$); also, the reduction in cellular survival rate was more pronounced for AgNPs2 ($p < 0.001$). This viability reduction might be a consequence of either cell death, proliferation suppression, or their combination [16]. AgNPs inhibition of cell proliferation and migration by activation of caspase 3 and 7 was previously reported [53]. To assess whether viability reduction was a result of cell death or suppression of proliferation, we performed Ki-67 immunofluorescent staining, which showed that at these concentrations, no proliferative active cells were detected (no Ki-67+ cells), while also cells with altered morphology (small, condensed nuclei) were observed, suggesting that viability reduction was a combination of both cytotoxic effect and proliferation suppression.

The effects of low concentrations were quite opposite. Both AgNPs1 and AgNPs2 decreased PAB levels ($p < 0.001$) at concentrations of 1, 0.1, and 0.05 $\mu\text{g}/\text{mL}$. Interestingly, the

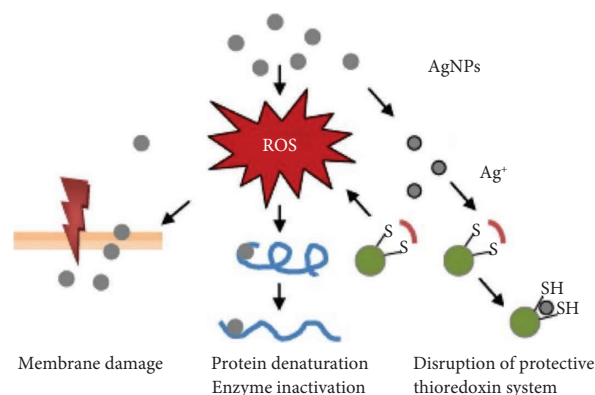


FIGURE 3: General mechanisms for the antimicrobial mode of action of AgNPs.

same concentrations had different effect on lipid peroxidation; AgNPs1 elevated lipid peroxidation products compared to control ($p < 0.01$ for 1 and 0.1 $\mu\text{g}/\text{mL}$), while only the lowest AgNPs2 concentration of 0.05 $\mu\text{g}/\text{mL}$ increased LPP ($p < 0.001$). The concentration of 0.1 $\mu\text{g}/\text{mL}$ had no effect and the concentration of 1 $\mu\text{g}/\text{mL}$ slightly, albeit insignificantly, reduced lipid peroxidation.

The effects on PAB levels could be explained by mild-free radicals' production which promptly activates enzymes involved in antioxidant defence. The enzymes can lower overall pro-oxidant/antioxidant balance to a certain extent, but at high concentrations, such as our determined MIC (14.35 $\mu\text{g}/\text{mL}$), their capacity is overcoming and pro-oxidant state occurs. *In vivo* study reported by Docea et al. [54] demonstrated that the subacute administration of AgNPs also lower pro-oxidant/antioxidant balance due to the activation of nonenzymatic (reduced GSH) and enzymatic (increased catalase activity) defence systems.

On the other hand, lipid peroxidation products are the result of interactions between ROS and polyunsaturated fatty acids (PUFA) [55]. Regarding the effects of lower AgNPs concentrations on LPP levels, two types of nanoparticles showed different trends. Larger AgNPs1 nanoparticles led to a small but consistent linear increase in lipid peroxidation (Figure 4). Furthermore, only the lowest (0.05 $\mu\text{g}/\text{mL}$) concentration of AgNPs2 increased LPP levels, while with an increase in concentration up to 1 $\mu\text{g}/\text{mL}$, LPP levels decreased. This discrepancy could be explained by the nanoparticle size, i.e., a similar trend was observed in the previously mentioned *in vivo* study [54]– PVP-coated nanoparticles that were larger increased TBARS dose-dependently, while EG-coated nanoparticles (smaller in size) increased TBARS at the lowest concentration, subsequently decreasing it at all higher concentrations, similar to AgNPs2. The authors explained that this difference was due to different coating materials; however, since in our experiment, the surface-stabilizing agent was the same for both types of AgNPs, the particle size should not be neglected. Another possible explanation is the interaction between nanosilver and enzymes involved in antioxidant defence, where it was shown that AgNPs sized 20 nm interact with catalase, thus suppressing its activity and disabling

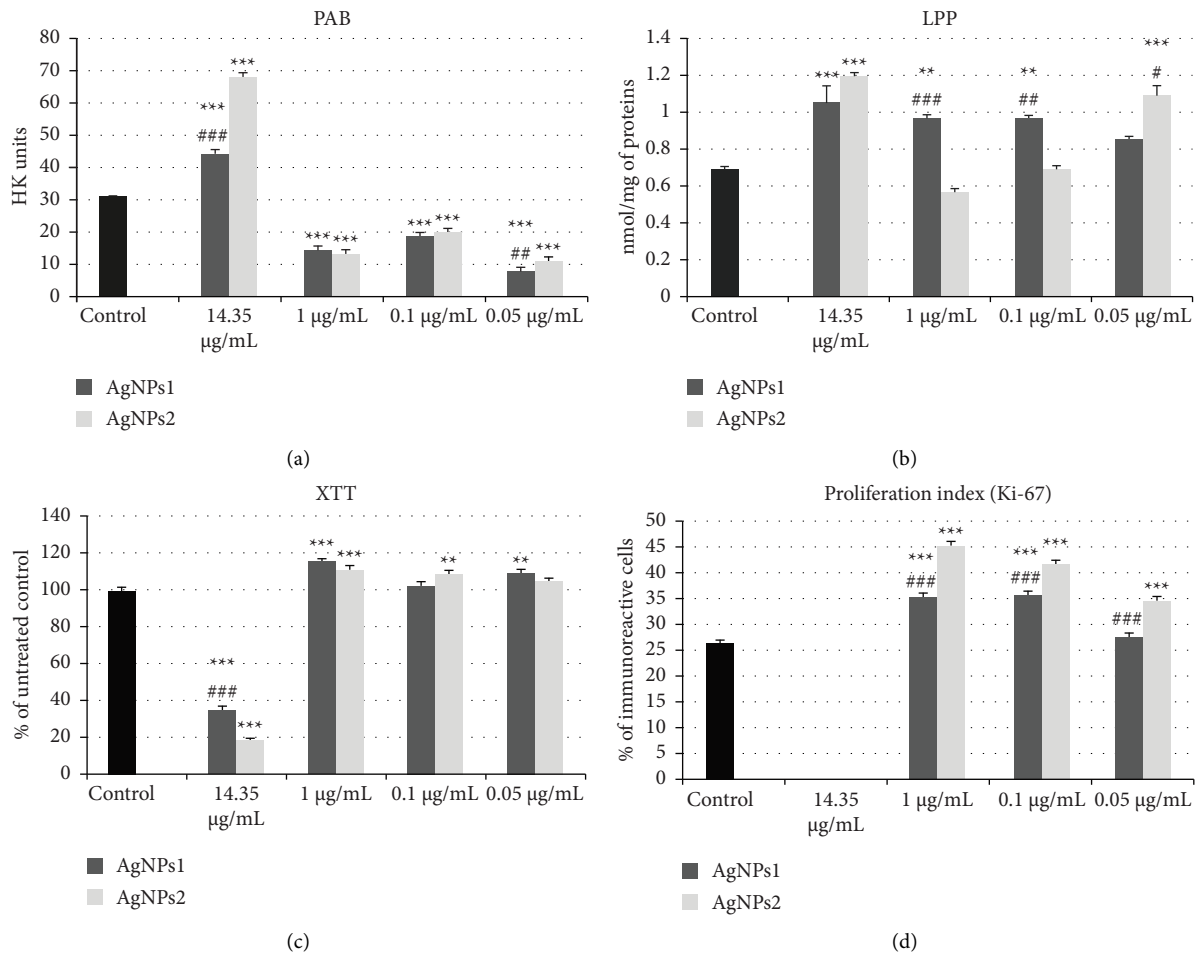


FIGURE 4: Prooxidant/antioxidant balance (PAB) (a), lipid peroxidation products (LPP) (b), cell viability (c), and the proliferation index of dermal fibroblast cells expressed as proliferation index (d) of both AgNPs1 and AgNPs2 and all treated concentrations ($n = 6$). *—control v.s. AgNPs1 or AgNPs2; #—AgNPs1 v.s. AgNPs2; */#— $p < 0.05$; **/#— $p < 0.01$; ***/###— $p < 0.001$.

antioxidative defence to a certain extent [56]. Additionally, smaller nanoparticles could display their effects beyond the cell membrane, i.e., the cellular uptake and interplay with mitochondria could be the cause of antioxidative enzymes activation, ROS quenching, and reduction of LPP levels at the lower applied concentrations [20, 57]. Bressan et al. demonstrated that AgNPs smaller than 20 nm enter human dermal fibroblasts by endocytosis, upon which they form aggregates in the close proximity of mitochondria and impair their function without altering other subcellular compartments. If ROS overaccumulate, the mitochondrial membrane could breakdown, leading to the release of mitochondrial antioxidative enzymes into the cytoplasm and ROS quenching or activation of regulatory genes involved in cellular defence, which results in overall cellular protection [58].

Consistent with this, it was shown that LPP production, depending on its extent, could not only lead to cellular damage but also display a protective effect [55]. Our results demonstrated that all three concentrations of both nanoparticles elevated XTT levels and the proliferation index (Ki-67⁺ cells) compared to the control (Figure 4(c), Figure 5).

Interestingly, for AgNPs2, this elevation was in inverse correlation with LPP, suggesting the previously mentioned activation of alternative regulatory genes with the pro-survival function. A mild increase in XTT levels was observed for AgNPs2 (statistically significant for 0.1 and 1 µg/mL, $p < 0.01$, and $p < 0.001$, respectively) and great concentration-dependent induction of cellular proliferation was observed for all three concentrations ($p < 0.001$). On the contrary, AgNPs1 led to slightly higher, albeit insignificant, increase in XTT levels compared to AgNPs2 (Figure 4(c)), and a statistically significant lower increase in the proliferation index compared to AgNPs2 ($p < 0.001$). Since XTT assay essentially represents a measure of the mitochondrial activity in living cells, i.e., not only the number of viable cells but also their metabolic activity, [59] higher proliferation rates after AgNPs2 could be a sign of activation of additional pro-survival pathways, rather than only mitochondrial that favour cellular proliferation. Our previous research also demonstrated that the proliferation ability of AgNPs is size dependent and probably mediated by ILGF-1 production in peripheral blood mononuclear cells [19]. In addition, other research studies also showed concentration- and size-

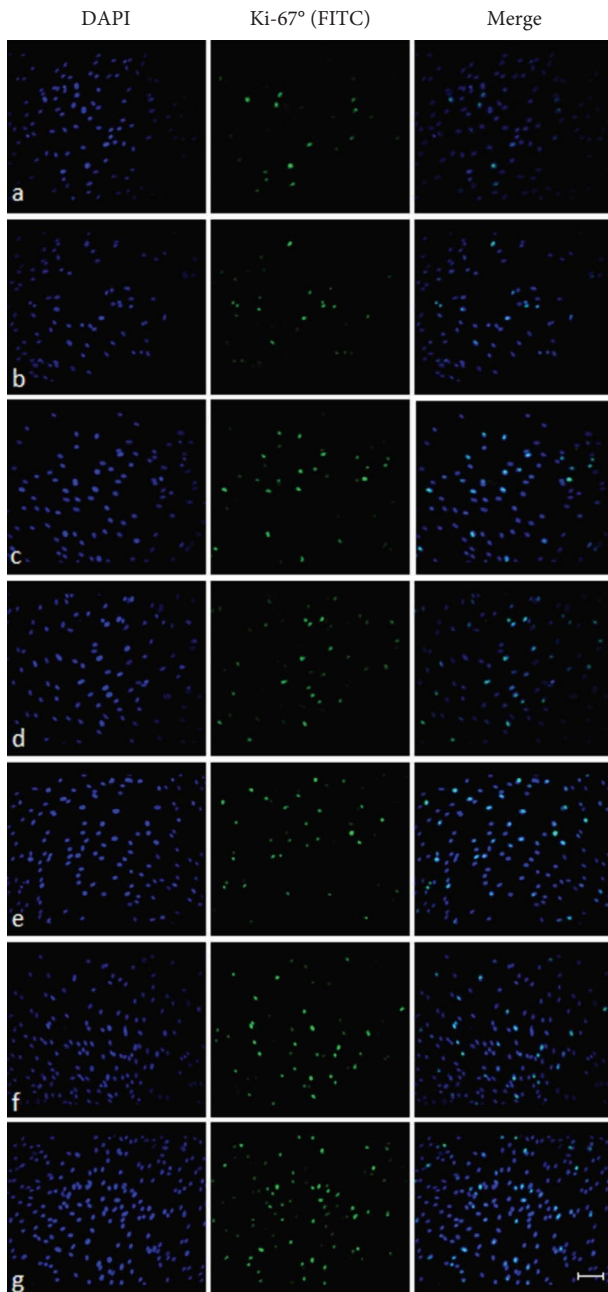


FIGURE 5: Ki-67 staining of control (untreated) fibroblast cells (a); cells treated with 0.05 (b), 0.1 (c), and 1 $\mu\text{g}/\text{mL}$ AgNPs1 (d); cells treated with 0.05 (e), 0.1, (f) and 1 $\mu\text{g}/\text{mL}$ AgNPs2 (g). The left panel shows DAPI stained cells; the middle panel (FITC) shows proliferative active Ki-67⁺ cells; the right panel shows merged DAPI + FITC photomicrographs. Scale bar = 100 μm .

dependant effects on the proliferation rates of human keratinocytes and dermal fibroblasts [2, 15, 60]. Similar to our results, high concentrations displayed a cytotoxic effect, while lower concentrations led to an increase in keratinocyte proliferation, without altering fibroblast proliferation rates. A positive effect on proliferation is mostly attributed to the suppression of proinflammatory pathways and the activation of anti-inflammatory pathways. Unlike these studies, we showed that lower concentrations also increase the

proliferation rate of human dermal fibroblasts and that this increase is more pronounced after treatment with smaller nanoparticles (Figure 5). We suppose that this effect is related to the activation of alternative pathways, but the exact mechanism remains to be elucidated.

4. Conclusion

The biological effects of different concentrations and sizes of two types of AgNPs synthesized by picosecond laser ablation of silver foil in a water solution of citric acid were examined in this study. Nanoparticles with good colloidal stability were obtained, whereas higher laser energy (12 mJ) produced overall smaller AgNPs ($15.3 \pm 4.6 \text{ nm}$) with higher concentration ($28.7 \pm 0.2 \mu\text{g}/\text{mL}$). High concentrations of these nanoparticles, AgNPs2, displayed a potent antibacterial effect against biofilm forming bacteria, as well as against *Staphylococcus aureus* and *Pseudomonas aeruginosa*. The same concentration also led to a strong pro-oxidant and cytotoxic effect with the complete inhibition of cell proliferation. However, when applied at lower doses, the antimicrobial effect was absent, but a positive effect on the cell proliferation and metabolic activity was observed, suggesting that different concentrations display a substantially opposite effect. Additionally, the low concentration showed an antioxidative effect probably due to the antioxidative enzymes activation. These findings could be of importance for the treatment of various conditions with essentially different pathophysiological mechanisms, ranging from dental biofilm inhibition and resistant dental infections, as well as proliferative conditions when applied at high concentrations, to atrophic and inflammatory conditions, when applied at low concentrations.

Data Availability

The data that support the findings of this study are available on request from the corresponding author.

Conflicts of Interest

The authors declare that there are no conflicts of interest.

Acknowledgments

The authors would like to acknowledge the following financial support for the research, authorship, and/or publication of this article. This work was supported by the Ministry of Education, Science and Technological Development of the Republic of Serbia (Contract number 451-03-47/2023-01/200017).

References

- [1] T. B. Asafa, R. A. Odediji, T. O. Salaudeen et al., "Physico-mechanical properties of emulsion paint embedded with silver nanoparticles," *Bulletin of Materials Science*, vol. 44, pp. 7–11, 2021.
- [2] A. Galandáková, J. Franková, N. Ambrožová et al., "Effects of silver nanoparticles on human dermal fibroblasts and

- epidermal keratinocytes," *Human & Experimental Toxicology*, vol. 35, no. 9, pp. 946–957, 2016.
- [3] M. Wypij, T. Jędrzejewski, J. Trzcńska-Wencel, M. Ostrowski, M. Rai, and P. Golińska, "Green synthesized silver nanoparticles: antibacterial and anticancer activities, biocompatibility, and analyses of surface-attached proteins," *Frontiers in Microbiology*, vol. 12, Article ID 632505, 2021.
- [4] I. Zorraquín-Peña, C. Cueva, B. Bartolomé, and M. V. Moreno-Arribas, "Silver nanoparticles against food-borne bacteria. Effects at intestinal level and health limitations," *Microorganisms*, vol. 8, no. 1, p. 132, 2020.
- [5] C. C. Fernandez, A. R. Sokolonski, M. S. Fonseca et al., "Applications of silver nanoparticles in dentistry: advances and technological innovation," *International Journal of Molecular Sciences*, vol. 22, no. 5, p. 2485, 2021.
- [6] I. X. Yin, J. Zhang, I. S. Zhao, M. L. Mei, Q. Li, and C. H. Chu, "The antibacterial mechanism of silver nanoparticles and its application in dentistry," *International Journal of Nanomedicine*, vol. 15, pp. 2555–2562, 2020.
- [7] X. F. Zhang, Z. G. Liu, W. Shen, and S. Gurunathan, "Silver nanoparticles: synthesis, characterization, properties, applications, and therapeutic approaches," *International Journal of Molecular Sciences*, vol. 17, no. 9, p. 1534, 2016.
- [8] N. Talank, H. Morad, H. Barabadi et al., "Bioengineering of green-synthesized silver nanoparticles: *In vitro* physico-chemical, antibacterial, biofilm inhibitory, anticoagulant, and antioxidant performance," *Talanta*, vol. 243, Article ID 123374, 2022.
- [9] C. Egbuna, V. K. Parmar, J. Jeevanandam et al., "Toxicity of nanoparticles in biomedical application: nanotoxicology," *Journal of Toxicology*, vol. 2021, Article ID 9954443, 21 pages, 2021.
- [10] Y. Li, T. Qin, T. Ingle et al., "Differential genotoxicity mechanisms of silver nanoparticles and silver ions," *Archives of Toxicology*, vol. 91, no. 1, pp. 509–519, 2017.
- [11] M. J. Piao, K. A. Kang, I. K. Lee et al., "Silver nanoparticles induce oxidative cell damage in human liver cells through inhibition of reduced glutathione and induction of mitochondria-involved apoptosis," *Toxicology Letters*, vol. 201, no. 1, pp. 92–100, 2011.
- [12] M. Bin-Jumah, M. Al, G. Albasher, and S. Alarifi, "Effects of green silver nanoparticles on apoptosis and oxidative stress in normal and cancerous human hepatic cells *in vitro*," *International Journal of Nanomedicine*, vol. 15, pp. 1537–1548, 2020.
- [13] H. Barabadi, M. Najafi, H. Samadian et al., "A systematic review of the genotoxicity and antigenotoxicity of biologically synthesized metallic nanomaterials: are green nanoparticles safe enough for clinical marketing?" *Medicina*, vol. 55, no. 8, pp. 439–444, 2019.
- [14] R. J. Holmila, S. A. Vance, S. B. King, A. W. Tsang, R. Singh, and C. M. Furdul, "Silver nanoparticles induce mitochondrial protein oxidation in lung cells impacting cell cycle and proliferation," *Antioxidants*, vol. 8, no. 11, p. 552, 2019.
- [15] X. Liu, P. Y. Lee, C. M. Ho et al., "Silver nanoparticles mediate differential responses in keratinocytes and fibroblasts during skin wound healing," *ChemMedChem*, vol. 5, no. 3, pp. 468–475, 2010.
- [16] Y. W. Huang, M. Cambre, and H. J. Lee, "The toxicity of nanoparticles depends on multiple molecular and physico-chemical mechanisms," *International Journal of Molecular Sciences*, vol. 18, no. 12, p. 2702, 2017.
- [17] C. Carlson, S. M. Hussain, A. M. L. Schrand, K. L. Hess, R. L. Jones, and J. J. Schlager, "Unique cellular interaction of silver nanoparticles: size-dependent generation of reactive oxygen species," *Journal of Physical Chemistry B*, vol. 112, no. 43, pp. 13608–13619, 2008.
- [18] J. Skalska, B. Dąbrowska-Bouta, M. Frontczak-Baniewicz, G. Sulkowski, and L. Strużyńska, "A low dose of nanoparticulate silver induces mitochondrial dysfunction and autophagy in adult rat brain," *Neurotoxicity Research*, vol. 38, no. 3, pp. 650–664, 2020.
- [19] G. Joksić, J. Stašić, J. Filipović, A. V. Šobot, and M. Trtica, "Size of silver nanoparticles determines proliferation ability of human circulating lymphocytes *in vitro*," *Toxicology Letters*, vol. 247, pp. 29–34, 2016.
- [20] R. de Lima, A. B. Seabra, and N. Durán, "Silver nanoparticles: a brief review of cytotoxicity and genotoxicity of chemically and biogenically synthesized nanoparticles," *Journal of Applied Toxicology*, vol. 32, no. 11, pp. 867–879, 2012.
- [21] P. Rama, A. Baldelli, A. Vignesh et al., "Antimicrobial, antioxidant, and angiogenic bioactive silver nanoparticles produced using *Murraya paniculata* (L.) jack leaves," *Nanomaterials and Nanotechnology*, vol. 12, Article ID 184798042110561, 2022.
- [22] M. R. Nagesh, N. Kumar, J. M. Khan et al., "Green synthesis and pharmacological applications of silver nanoparticles using ethanolic extract of *Salacia chinensis* L.," *Journal of King Saud University Science*, vol. 34, no. 7, Article ID 102284, 2022.
- [23] S. M. Gamboa, E. R. Rojas, and V. V. Martínez, "Synthesis and characterization of silver nanoparticles and their application as an antibacterial agent," *International Journal of Biosensors & Bioelectronics*, vol. 5, pp. 166–173, 2019.
- [24] B. Perito, E. Giorgetti, P. Marsili, and M. Muniz-Miranda, "Antibacterial activity of silver nanoparticles obtained by pulsed laser ablation in pure water and in chloride solution," *Beilstein Journal of Nanotechnology*, vol. 7, pp. 465–473, 2016.
- [25] L. Krce, M. Šprung, A. Maravić et al., "Bacteria exposed to silver nanoparticles synthesized by laser ablation in water: modelling *E. coli* growth and inactivation," *Materials*, vol. 13, no. 3, p. 653, 2020.
- [26] L. Krce, M. Šprung, T. Rončević et al., "Probing the mode of antibacterial action of silver nanoparticles synthesized by laser ablation in water: what fluorescence and AFM data tell us," *Nanomaterials*, vol. 10, no. 6, p. 1040, 2020.
- [27] X. C. Jiang, C. Y. Chen, W. M. Chen, and A. B. Yu, "Role of citric acid in the formation of silver nanoplates through a synergistic reduction approach," *Langmuir*, vol. 26, no. 6, pp. 4400–4408, 2010.
- [28] R. La Spina, D. Mehn, F. Fumagalli et al., "Synthesis of citrate-stabilized silver nanoparticles modified by thermal and pH preconditioned tannic acid," *Nanomaterials*, vol. 10, p. 2031, 2020.
- [29] B. Vuković, M. Milić, B. Dobrošević et al., "Surface stabilization affects toxicity of silver nanoparticles in human peripheral blood mononuclear cells," *Nanomaterials*, vol. 10, no. 7, p. 1390, 2020.
- [30] M. Khubchandani, N. R. Thosar, S. Dangore-Khasbage, and R. Srivastava, "Applications of silver nanoparticles in pediatric dentistry: an overview," *Cureus*, vol. 14, no. 7, Article ID e26956, 2022.
- [31] L. Sedghi, V. DiMassa, A. Harrington, S. V. Lynch, and Y. L. Kapila, "The oral microbiome: role of key organisms and complex networks in oral health and disease," *Periodontology 2000*, vol. 87, no. 1, pp. 107–131, 2021.
- [32] J. Harris-Ricardo, L. Fang, A. Herrera-Herrera et al., "Bacterial profile of the supragingival dental biofilm in children

- with deciduous and early mixed dentition using next generation sequencing (HOMINGS) technique,” *Enfermedades Infecciosas y Microbiología Clínica*, vol. 37, no. 7, pp. 448–453, 2019.
- [33] I. Prada, P. Micó-Muñoz, T. Giner-Lluesma, P. Mico-Martinez, N. Collado-Castellano, and A. Manzano-Saiz, “Influence of microbiology on endodontic failure. Literature review,” *Medicina Oral, Patología Oral y Cirugía Bucal*, vol. 24, no. 3, pp. e364–e372, 2019.
- [34] C. A. Schneider, W. S. Rasband, and K. W. Eliceiri, “NIH Image to ImageJ: 25 years of image analysis,” *Nature Methods*, vol. 9, no. 7, pp. 671–675, 2012.
- [35] N. W. Roehm, G. H. Rodgers, S. M. Hatfield, and A. L. Glasebrook, “An improved colorimetric assay for cell proliferation and viability utilizing the tetrazolium salt XTT,” *Journal of Immunological Methods*, vol. 142, no. 2, pp. 257–265, 1991.
- [36] O. H. Lowry, N. J. Rosebrough, A. L. Farr, and R. Randall, “Protein measurement with the Folin phenol reagent,” *Journal of Biological Chemistry*, vol. 193, no. 1, pp. 265–275, 1951.
- [37] D. H. Alamdari, K. Paletas, T. Pegiou, M. Sarigianni, C. Befani, and G. Koliakos, “A novel assay for the evaluation of the prooxidant-antioxidant balance, before and after antioxidant vitamin administration in type II diabetes patients,” *Clinical Biochemistry*, vol. 40, no. 3-4, pp. 248–254, 2007.
- [38] D. Tsikas, “Assessment of lipid peroxidation by measuring malondialdehyde (MDA) and relatives in biological samples: analytical and biological challenges,” *Analytical Biochemistry*, vol. 524, pp. 13–30, 2017.
- [39] K. Anandalakshmi, J. Venugobal, and V. Ramasamy, “Characterization of silver nanoparticles by green synthesis method using *Pedaliium murex* leaf extract and their antibacterial activity,” *Applied Nanoscience*, vol. 6, no. 3, pp. 399–408, 2016.
- [40] R. H. Müller, C. Jacobs, and O. Kayser, “Nanosuspensions as particulate drug formulations in therapy: rationale for development and what we can expect for the future,” *Advanced Drug Delivery Reviews*, vol. 47, no. 1, pp. 3–19, 2001.
- [41] T. Bruna, F. Maldonado-Bravo, P. Jara, and N. Caro, “Silver nanoparticles and their antibacterial applications,” *International Journal of Molecular Sciences*, vol. 22, no. 13, p. 7202, 2021.
- [42] H. Barabadi, F. Mojab, H. Vahidi et al., “Green synthesis, characterization, antibacterial and biofilm inhibitory activity of silver nanoparticles compared to commercial silver nanoparticles,” *Inorganic Chemistry Communications*, vol. 129, Article ID 108647, 2021.
- [43] R. S. Hamida, M. A. Ali, D. A. Goda, M. I. Khalil, and M. I. Al-Zaban, “Novel biogenic silver nanoparticle-induced reactive oxygen species inhibit the biofilm formation and virulence activities of methicillin-resistant *Staphylococcus aureus* (MRSA) strain,” *Frontiers in Bioengineering and Biotechnology*, vol. 8, p. 433, 2020.
- [44] Y. G. Yuan, Q. L. Peng, and S. Gurunathan, “Effects of silver nanoparticles on multiple drug-resistant strains of *Staphylococcus aureus* and *Pseudomonas aeruginosa* from mastitis-infected goats: an alternative approach for antimicrobial therapy,” *International Journal of Molecular Sciences*, vol. 18, no. 3, p. 569, 2017.
- [45] A. A. Menazea, “Femtosecond laser ablation-assisted synthesis of silver nanoparticles in organic and inorganic liquids medium and their antibacterial efficiency,” *Radiation Physics and Chemistry*, vol. 168, Article ID 108616, 2020.
- [46] J. K. Pandey, R. K. Swarnkar, K. K. Soumya et al., “Silver nanoparticles synthesized by pulsed laser ablation: as a potent antibacterial agent for human enteropathogenic gram-positive and gram-negative bacterial strains,” *Applied Biochemistry and Biotechnology*, vol. 174, pp. 1021–1031, 2014.
- [47] I. Zorraquín-Peña, C. Cueva, D. González de Llano, B. Bartolomé, and M. V. Moreno-Arribas, “Glutathione-stabilized silver nanoparticles: antibacterial activity against periodontal bacteria, and cytotoxicity and inflammatory response in oral cells,” *Biomedicine*, vol. 8, no. 10, p. 375, 2020.
- [48] L. F. Espinosa-Cristóbal, G. A. Martínez-Castañón, R. E. Martínez-Martínez, J. Loyola-Rodríguez, and F. Ruiz, “Antibacterial effect of silver nanoparticles against *Streptococcus mutans*,” *Materials Letters*, vol. 63, no. 29, pp. 2603–2606, 2009.
- [49] Q. Zhang, Y. Hu, C. M. Masterson et al., “When function is biological: discerning how silver nanoparticle structure dictates antimicrobial activity,” *Science*, vol. 25, no. 7, Article ID 104475, 2022.
- [50] T. C. Dakal, A. Kumar, R. S. Majumdar, and V. Yadav, “Mechanistic basis of antimicrobial actions of silver nanoparticles,” *Frontiers in Microbiology*, vol. 7, p. 1831, 2016.
- [51] A. N. Kodintcev, “Characterization and potential applications of silver nanoparticles: an insight on different mechanisms,” *Chimica Techno Acta*, vol. 9, no. 4, Article ID 20229402, 2022.
- [52] M. A. Quinteros, V. Cano Aristizábal, P. R. Dalmasso, M. Paraje, and P. Páez, “Oxidative stress generation of silver nanoparticles in three bacterial genera and its relationship with the antimicrobial activity,” *Toxicology in Vitro*, vol. 36, pp. 216–223, 2016.
- [53] L. Xu, Y. Y. Wang, J. Huang, C. Y. Chen, Z. X. Wang, and H. Xie, “Silver nanoparticles: synthesis, medical applications and biosafety,” *Theranostics*, vol. 10, no. 20, pp. 8996–9031, 2020.
- [54] A. O. Docea, D. Calina, A. M. Buga et al., “The effect of silver nanoparticles on antioxidant/pro-oxidant balance in a murine model,” *International Journal of Molecular Sciences*, vol. 21, no. 4, p. 1233, 2020.
- [55] M. Morales and S. Munné-Bosch, “Malondialdehyde: facts and artifacts,” *Plant Physiology (Washington D C)*, vol. 180, no. 3, pp. 1246–1250, 2019.
- [56] W. Liu, I. Worms, and V. I. Slaveykova, “Interaction of silver nanoparticles with antioxidant enzymes,” *Environmental Sciences: Nano*, vol. 7, no. 5, pp. 1507–1517, 2020.
- [57] E. Bressan, L. Ferroni, C. Gardin et al., “Silver nanoparticles and mitochondrial interaction,” *International Journal of Dentistry*, vol. 2013, Article ID 312747, 8 pages, 2013.
- [58] H. C. Lee, P. H. Yin, C. Y. Lu, C. W. Chi, and Y. H. Wei, “Increase of mitochondria and mitochondrial DNA in response to oxidative stress in human cells,” *Biochemical Journal*, vol. 348, no. 2, pp. 425–432, 2000.
- [59] Q. Gu, E. Cuevas, S. F. Ali et al., “An alternative *in vitro* method for examining nanoparticle-induced cytotoxicity,” *International Journal of Toxicology*, vol. 38, no. 5, pp. 385–394, 2019.
- [60] J. Tian, K. K. Wong, C. M. Ho et al., “Topical delivery of silver nanoparticles promotes wound healing,” *ChemMedChem*, vol. 2, no. 1, pp. 129–136, 2007.